2013 International Conference on Indoor Positioning and Indoor Navigation, 28-31st October 2013

Light-Matching: a new Signal of Opportunity for Pedestrian Indoor Navigation

A.R. Jiménez, F. Zampella, F. Seco
Centre for Automation and Robotics (CAR)
Consejo Superior de Investigaciones Científicas (CSIC)-UPM
Ctra. Campo Real km 0.2, 28500 La Poveda, Arganda del Rey, Madrid, Spain
e-mail: {antonio.jimenez, francisco.zampella, fernando.seco}@csic.es
web: http://www.car.upm-csic.es/lopsi

***Abstract*—This paper presents a new indoor location concept named *Light-matching* which uses the perceived gradient in the illumination from unmodified indoor lights to achieve accurate physical location. The proposed method does not require any illumination calibration, just the pre-storage of the position and size of all lights in a building, irrespective of their current on/off state. The *Light-matching* method also requires the estimation of the relative displacement and orientation change of a person which is done by inertial Pedestrian Dead-Reckoning (PDR). Even from an initially unknown location and orientation, whenever the person passes below a switched-on light spot, the location likelihood is iteratively updated until it potentially converges to an unimodal probability density function. The time to converge to an unimodal position hypothesis depends on the number of lights detected and the asymmetries/irregularities of light distributions. The light-matching technique can be used alone or in cooperation with other signals of opportunity (WiFi, Magnetometers or Map-matching) to obtain a continuous high accuracy indoor localization system. This paper presents the basic description of the light-matching concept, the implementation details using a particle filter, and the evaluation of the method by simulation. The performance of the integrated solution can achieve a localization error lower than 1 m in most of the cases.**

***Keywords*—Indoor localization, Signals of opportunity, Light/Illumination, Pedestrian dead-reckoning, Smartphone.**

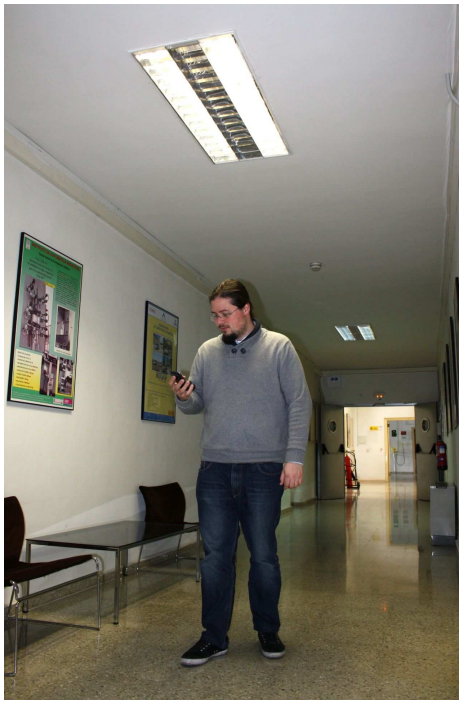

Fig. 1. Fine-grained location of people indoors using the *Light-matching* approach. When a person passes under any standard/unmodified light spot, then his location likelihood is updated. Inertial-based Pedestrian Dead-Reckoning (PDR) is used as a motion model to propagate his location likelihood. Other available sensors (magnetometer), context information (map) or signal of opportunity (WiFi) can be used as a backup or to improve/guarantee an unimodal location estimation.

I. Introduction

Indoor localization is still an open problem. Many different approaches using distinct technologies have been proposed to obtain a usability similar to GPS outdoors [1], [2], [3]. The most difficult challenge for pedestrian navigation is to find an accurate-enough indoor location method, valid for extended areas, robust to environmental conditions, and at the same time as simple as possible. Two main approaches can be used for the location of persons indoors: 1) Solutions that rely on the existence of a network of receivers or emitters placed at known locations (beacon-based solutions or Local Positioning Systems-LPS) [4], [5], [6], and 2) Solutions that mainly rely on dead-reckoning methods with sensors only installed on the person to be located (beacon-free solutions, or Pedestrian Dead Reckoning-PDR) [7], [8], [9], [10]. The current tendency is the hybridization of both approaches [11], [12].

The use of *signals of opportunity* for the localization of persons indoors is a recent and very promising approach, specially from the usability point of view. Signals of opportunity are those not originally meant for localization purposes but which are freely available most of the time in standard unmodified spaces. Some common signals of opportunity are: telephony, FM/TV broadcast, WiFi, Bluetooth, magnetic fingerprints, illumination, pressure, temperature, among others [13], [14]. In order to avoid the use of specific hardware, a smart-phone could be used to register these signals. This approach has the advantage of not requiring the installation of any ad-hoc infrastructure.

One of those signals of opportunity is the *light intensity* from standard light sources. The estimation of the position of a person indoors using unmodified artificial lights (e.g. fluorescent lights) has received little attention in the research community. A few authors [15], [16] used unmodified light

978–1–46773–1954–6/12$31.00

signals to perform room-level localization using fingerprinting approaches to infer in which room the user could be located. They assume that the illumination intensity and/or ambient color is different among particular rooms. This approach has the limitations of providing just a symbolic positioning (i.e a poor physical location accuracy), and the necessity to perform frequent re-calibrations to update the measurement models, since lighting conditions can change.

Another author uses the light intensity variations from standard fluorescent lights to estimate the relative displacement of a person while walking [17]. The estimation is based on how the sensed illumination changes as the distance from the user to the light source varies. In this work the user has a small solar panel embedded on the clothes as the illumination sensor. The main drawbacks of this approach are: illuminance depends on the orientation of the receiver, influence of close-by windows with natural light, sensitivity to the light rated power (different behaviour e.g. for 30 or 60 Watts lights), influence of aging of lights, dust accumulation, influence of the reflectivity of surrounding objects, diffusers, etc. Additionally, as the method estimates the relative traveled distance, it has to be integrated with an absolute positioning system (RFID-based in this case) in order to be able to estimate the user location.

There exists other approaches using special indoor lights for absolute localization, which are called *light-communication* [18], [19], some of which are on the market (bytelight.com). However these approaches require the modification of the infrastructure, by adding electronic modulators of the current that energizes the lights. In this manner each particular light emits or "communicates" a unique identification, or alternatively, its position. This is a similar concept to infrastructure-based LPS localization that is far from the unmodified approach that we propose in this paper.

In this paper we present a concept termed as *Light-matching* which is a new way to use the information coming from unmodified lights in indoor environments (see Fig. 1) to achieve accurate physical location without the need of any light-state calibration. As in other matching techniques, we need to know the 2D positions, size and orientation of all lights in a building, however the current lighting state (if they are on or off) is not needed. The light-matching method also requires the use of an inertial Dead-Reckoning (PDR) method to estimate the displacement and changes in orientation of the person while is walking. Even from an initially unknown location and orientation, whenever the person passes below an switched-on light spot, the location likelihood is iteratively updated until the likelihood potentially converges to a unimodal probability density function. The time to converge to an unimodal position hypothesis depends on the number of lights detected and the asymmetries/irregularities of light distributions. This approach can be used in cooperation with other signals of opportunity (WiFi, Magnetometers or map-maching) to obtain an even better indoor localization accuracy.

This paper presents the basic description of the light-matching concept (section II), the implementation details (section III), and several simulated tests (section IV). Finally, in the last section, we give some conclusions.

II. Light-Matching Concept

This section explains the basic Light-matching idea, i.e. how to use unmodified lights to determine the user's location. We also analyze the localization convergence, measured as the change in the number of location hypothesis, and how it is influenced by the number of lights in a building and the number of detections.

A. Basic Light-Matching Idea

The Light-Matching idea is very simple. If we know exactly where all the lights in a building are located (2D position, size and orientation of each light in each floor), and we assume that we are able to detect when a person has passed under a light spot, then we can infer that under a light detection the person can be located under any of the lights in that floor plant. So, under an unknown initial position and orientation, a light detection implies as many local hypothesis as the number of lights in a building. These multi-modal location hypotheses are propagated according to a motion model that can be estimated with pedestrian dead-reckoning techniques. After a second light detection, the current multi-modal hypothesis located under any light spot will persist, and the rest of the hypothesis will be discarded. This process of hypothesis propagation (motion model) and hypothesis update at light detections (measurement model), finally can converge to an unimodal hypothesis that represents the true location of the person. This concept can be straightforward implemented using a Bayesian approach with a particle filter implementation, giving each particle a state, X, consisting of a location and an orientation ($X = \{x, y, z, \theta\}$).

In Fig. 2 the Light-Matching concept is explained with an example. We illustrate the case of a person that is walking straight (magenta arrow) in a simplified building floor with only two light spots (yellow circles) separated by a distance *2d*. We use several particles to represent the likelihood of the location hypothesis, as well as their orientations (represented by a short tail at each particle). At the beginning (t=0), Fig. 2a, we do not know where the person is located so the particles are spread in the floor-plan with a uniform orientation distribution. When the user moves under a light and detects it for the first time (t=k), then we know that he can only be under any of the two lights in the building. This is represented by a double cluster of particles that represent two local unimodal hypothesis (Fig. 2b). Note that these two hypotheses have not any preferred orientation (i.e. uniform distribution). While the user walks straight a distance d, at time t=k+1 (Fig. 2c), and another distance d at t=k+2, the particles separate from the light centers according to their individual orientation creating a circular ring for each light position (Fig. 2d). At this time (t=k+2) a second light is detected, which causes an update that reinforce the likelihood under the two lights and eliminates the remaining particles (Fig. 2e). Note that this two hypothesis have, apart from distinctive locations, two defined orientations (particles at upper cluster point "North", and those at the lower cluster point "South"). If the user continues his straight motion both clusters are moved according to the PDR estimation. We know that the upper hypothesis is the correct one (we advanced the real trajectory in Fig. 2a) but without any prior knowledge both hypothesis are equally valid, one that corresponds to a

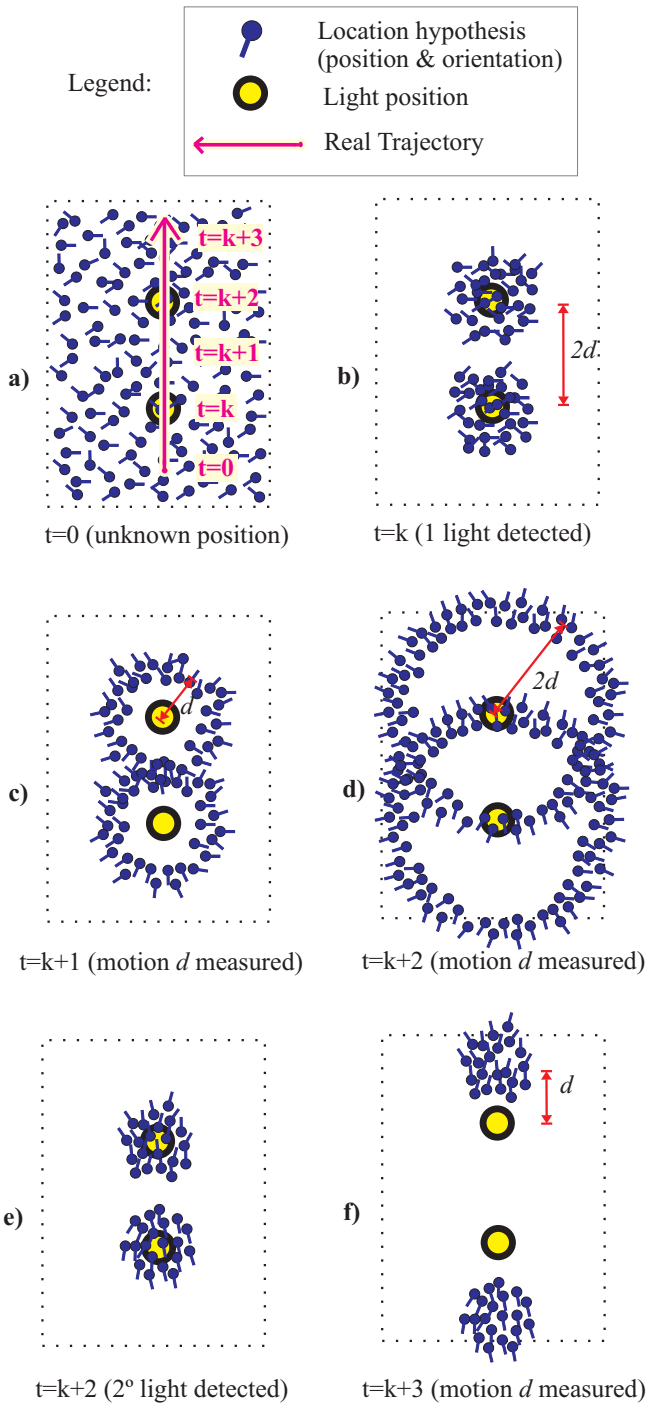

Fig. 2. Light-Matching concept applied to estimate the location and heading of a person. Example of how the uncertainty in the estimation is reduced when the person gets under two lights while walking straight in an indoor area. a) Initially (t=0) there is no information about the location of the person in the area (represented by multiple location hypothesis at several places and with different orientations). b) The person is under a light, so he must be at any of the light locations. c) the persons moves a distance *d* since last light detection (measured by PDR). d) and e) after moving straight a distance *d* at time t=k+2, the person is under another light. f) After this second light detection there are only two main cluster of location hypothesis with well-defined position and orientation (one of those corresponds to the true location).

Number of Lights (n_{lights})	Number of Detections (n_{det})	Number of Hypotheses (n_{hyp})
1	0	∞
	1	n_{quad}
2	0	∞
	1	$2 \cdot n_{\text{quad}}$
	2	2
3	0	∞
	1	$3 \cdot n_{\text{quad}}$
	2	4
	3	2
4	0	∞
	1	$4 \cdot n_{\text{quad}}$
	2	6
	3	4
	4	2
5	0	∞
	1	$5 \cdot n_{\text{quad}}$
	2	8
	3	6
	4	4
	5	2

TABLE I. DEPENDANCE OF THE NUMBER OF LOCATION HYPOTHESIS WITH THE NUMBER OF LIGHTS PRESENT AND THE NUMBER OF LIGHTS DETECTED (CASE OF LIGHTS ALIGNED AND A STRAIGHT PATH).

straight path from South to North starting below, and another from North to South starting above in the floor map.

B. The Total Number of Hypotheses: Influence of the Number of Lights and Detections

In this paper we are using the term "*hypothesis*" to refer to any unimodal location likelihood or equivalently, to any cluster of particles that share a similar position and orientation. Each particle itself, although it is also an hypothesis, only represents a sample of the probability density function of the overall distribution.

In the example of the previous subsection (Sec. II-A and Fig. 2), consisting of two lights in a floor, we ended, after passing under two lights, that the number of *hypothesis* was two. Curiously, this number was equal to the number of lights. In general, if the number of lights in the building, n_{lights}, increases it is expected that the number of hypotheses, n_{hyp}, will grow proportionally after the first light detection. So, $n_{\text{hyp}} \propto n_{\text{lights}}$ for only one light detection. If the person moves, from that location, the particles in each hypothesis will be spread forming rings of particles centered in each light position (as in Fig. 2c and d). If we consider that we can split each ring of particles in several quadrants, for example 4 or 8 quadrants, corresponding to angle ranges of 90 or 45 degrees, respectively, then we can consider that each ring of particles contains n_{quad} hypothesis (being for example $n_{\text{quad}} = 8$). So, in general we can say that the number of hypotheses after just one light detection is equal to the number of light multiplied by the number of quadrants, i.e. $n_{\text{hyp}} = n_{\text{lights}} \cdot n_{\text{quad}}$.

The grow of the number of hypotheses with the numbers of lights in a building, which is an undesirable feature, however can be alleviated by the number of light detections, n_{det}, that

occur while the person is walking indoors. In table I it is shown the systematic calculation of the total number of hypotheses for a different number of aligned lights installed in a corridor in a building, and for different number of detections while a person is walking straight in each case. We see that when the number of detections is larger that two, then the number of hypotheses begin to diminish proportionally. The following formula can be generalized for this series of data:

$$n_{\text{hyp}} = \begin{cases} 2 \cdot (n_{\text{lights}} + 1) - 2 \cdot n_{\text{det}} & if n_{\text{det}} \geq 2 \\ n_{\text{lights}} \cdot n_{\text{quad}} & if n_{\text{det}} = 1 \\ \infty & if n_{\text{det}} = 0 \end{cases}, \quad (1)$$

which although is only valid for the case of a person moving straight, it gives us a concrete idea of how the number of hypotheses depend on the number of lights in the building and the number of light detections. From this case, we can see that visiting half of the lights in the building ($n_{\text{det}} = n_{\text{lights}}/2$) the number of hypotheses is similar to the number of lights ($n_{\text{hyp}} = n_{\text{lights}} + 2$). Even visiting all the lights in a building ($n_{\text{det}} = n_{\text{lights}}$) the minimum number of hypotheses is still 2 ($n_{\text{hyp}} = 2$). This means that additional methods to prune the hypothesis are needed.

C. Pruning the number of Hypotheses

In principle one of the main drawbacks of the Light-matching concept is that it generates multiple hypothesis (proportional to the number of lights, eq.1) and therefore does not provide a unique location hypothesis. Although this is in general true the Light-matching approach can frequently converge to a unique location hypothesis under one or several of the following common circumstances:

- *Using the Earth magnetic field.*
- *Existence of Irregular Light Distributions.*
- *In cooperation with other sensors/information.*

A future extension of this work into a more detailed journal manuscript will explain how these common circumstances help to prune the number of hypotheses.

III. Light-Matching Implementation in a Pedestrian Localization Framework

In this section we give the implementation details of our localization methodology. We use a Bayesian filter, implemented with a Particle Filter (PF), to integrate the measurements coming from the light detections, as well as any other information that could be available (Magnetometer, Wifi, GPS, Map, etc). The motion information is mainly provided by a PDR subsystem that is also integrated in the same framework (see Fig. 3).

A. Particle Filter-based Pedestrian Localization Framework

In our PF implementation we use a *state vector*, X, composed of 4 components: $X = \{r_x, r_y, r_z, \theta\}$. The first three terms represent the 3D position, $r = \{r_x, r_y, r_z\}$, and the last term θ is the heading with respect an arbitrary-selected local navigation frame. We use a classical recursive

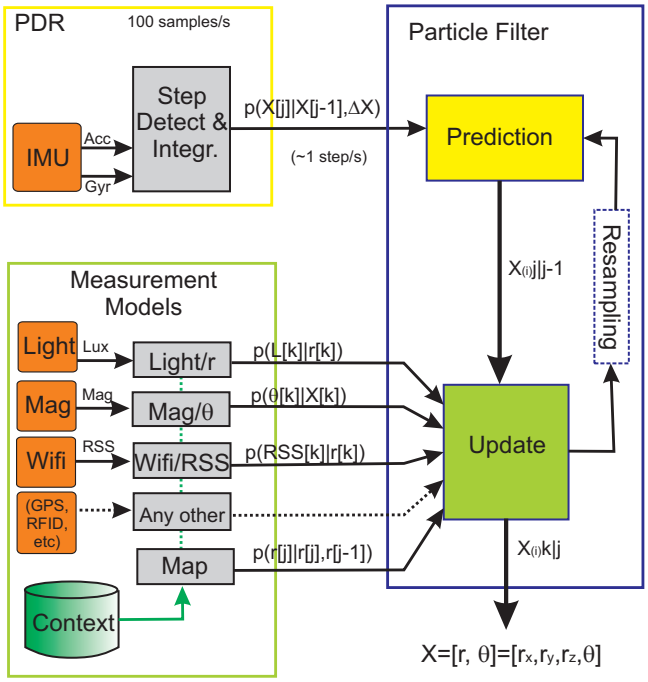

Fig. 3. General Pedestrian Localization Framework based on a Particle Filter implementation. This approach is used in this paper to include the light detections and the Light-matching measurement model.

prediction of the state vector, followed by an *update* of the state when a measurement is available. Occasional *resamplings* are performed when a degeneration of the particles is detected [20]. Next it is detailed each of these prediction and update stages.

1) PDR-based Prediction: A *prediction* is performed whenever an step j is detected with the PDR subsystem. This PDR module estimates the PDR inter-step changes, $\Delta X[j] = \{\Delta r_x[j], \Delta r_y[j], \Delta r_z[j], \Delta\theta[j]\}$, from the last step $j-1$ to the current step j, using a Kalman-based INS algorithm with ZUPT updates [21]. We preferably use a foot-mounted INS integration method because it is possible to accurately estimate the changes in the 3D position and the foot heading with respect to the last step pose. In Fig. 4 these inter-step changes are depicted, as well as the trajectory of the right foot of a pedestrian after some step detections.

The prediction stage in the PF moves all the particles, $X^{(i)}$, for $i = 1 \ldots N$, from the last detected step at time $t_{\text{PDR}}[j-1]$, according to the estimated $\Delta X[j]$ at current step at time $t_{\text{PDR}}[j]$. This propagation (movement and rotation) of the particles states also includes the addition of some random state values, that represent the uncertainty of the movement model, i.e.

$$X^{(i)}[j] = X^{(i)}[j-1] + f(\Delta X[j], n_{step}, \theta^{(i)}[j-1]), \quad (2)$$

where $n_{step} \sim \mathcal{N}(0, P[j])$, i.e. represents the covariance error model of the PDR prediction. As the inter-step changes are always measured in the reference frame of the previous step, then it is needed to transform the ΔX estimations to

the local localization frame. The function f includes that non-linear Z-axis rotation operation by $\theta^{(i)}[j-1]$ to transform the ΔX PDR estimations, referenced in the frame of the last step detection $(j-1)$, to the local reference frame.

$$f(\Delta X[j], n_{step}, \theta^{(i)}[j-1]) =$$

$$\begin{bmatrix} \cos(\theta^{(i)}[j\text{-}1]) & -\sin(\theta^{(i)}[j\text{-}1]) & 0 & 0 \\ \sin(\theta^{(i)}[j\text{-}1]) & \cos(\theta^{(i)}[j\text{-}1]) & 0 & 0 \\ 0 & 0 & 1 & 0 \\ 0 & 0 & 0 & 1 \end{bmatrix} \times \tag{3}$$

$$\left(\begin{bmatrix} \Delta r_x[j] \\ \Delta r_y[j] \\ \Delta r_z[j] \\ \Delta\theta[j] \end{bmatrix} + \sqrt{P[j]} \cdot \text{randn}^{(i)}(4,1) \right),$$

where "randn$^{(i)}(4,1)$" is 4-value column of normally distributed pseudorandom numbers.

2) Measurement-based Update: The *update* stage to refine the predicted state of the particles is computed whenever a measurement k is received at time $t_{\text{meas}}[k]$. Note the different notation (j and k) to represent the index of steps and measurement occurrences, respectively, which in general occur at different time instants ($t_{\text{PDR}}[j]$ and $t_{\text{meas}}[k]$). A different measurement model exists for each type of measurement (Light-matching, magnetometer, Wifi, Map-maching, etc). According to these models the weight of each particle, representing the likelihood of the user being at a certain position and orientation, is changed:

$$w^{(i)}[k] = w^{(i)}[k-1] \cdot p(z[k]|\hat{X}^{(i)}[k]) \cdot \alpha, \tag{4}$$

where $p(z[k]|\hat{X}^{(i)}[k])$ is the likelihood function obtained from the measurement $z[k]$ when the state of the particles at time $t_{\text{meas}}[k]$ is estimated to be $\hat{X}^{(i)}[k]$. The term α is a normalization factor to guarantee that the sum of all probabilities is equal to 1.

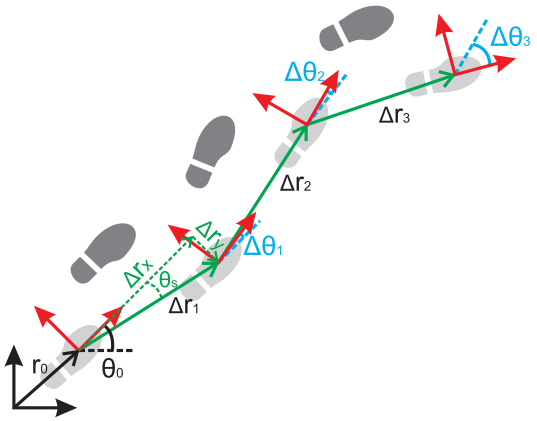

Fig. 4. Reconstruction of the position using the step displacements (green) and heading changes (blue) obtained from PDR and starting from the initial position r_0 and heading θ_0

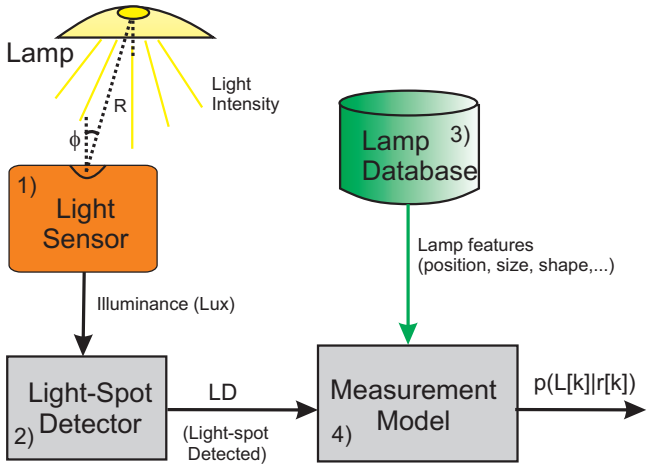

Fig. 5. Components in the measurement subsystem of the Light-matching approach: 1) Illumination sensor, 2) Light spot detector, 3) Lamp database, and 4) Measurement model.

Note that as the state of the particles are only sampled at step detections (i.e. at times: $t_{\text{PDR}}[j]$ for $j = 1 \ldots \text{Num}_{\text{steps}}$), then we must interpolate the particles' state at times of measurement ($t_{\text{meas}}[k]$), in order to obtain $\hat{X}[k]$. So $\hat{X}[k]$ is an approximation of the position and orientation of the particles assuming a constant velocity between the step points, as:

$$\hat{X}^{(i)}[k] = X^{(i)}[j-1] + \gamma \cdot (X^{(i)}[j] - X^{(i)}[j-1]), \tag{5}$$

where γ is the interpolation weight:

$$\gamma = \frac{(t_{\text{meas}}[k] - t_{\text{PDR}}[j-1])}{(t_{\text{PDR}}[j] - t_{\text{PDR}}[j-1])}. \tag{6}$$

The output of the filter, which is computed at the step detection rate (aprox. 1 Hz), uses the states for the last detected step, $X^{(i)}[j] = \{r_x^{(i)}[j], r_y^{(i)}[j], r_z^{(i)}[j], \theta^{(i)}[j]\}$, and the weights updated with the last measurement, $w^{(i)}[k]$, to estimate the localization and orientation of the user:

$$X_{(j,k)} = \sum_{i=1}^{N} X^{(i)}[j] \cdot w^{(i)}[k]. \tag{7}$$

B. Light-Matching Measuring Components

The measurement subsystem of the Light-matching approach consists basically of 4 components: 1) a *sensor* to capture the ambient illumination, 2) a *light spot detector*, which is a signal processing block to analyze illumination changes in order to deduce when a person has walked under a light, 3) a *database* including the coordinates and features of all lamps in a building, and 4) a *measurement model*, $p(L[k]|r[k])$, that represents the probability of detecting a light while the user is at a certain location r at time $t_{\text{meas}}[k]$. This components are depicted in Fig. 5, and explained in more detail next.

1) Illumination at the Sensor: There are different illumination technologies for indoor use, such as, incandescent lights (tungsten bulbs, halogen), discharge lamps (fluorescent, Xenon,...), and LED lamps. The Light-matching concept is

independent of the type of technology employed; the only requirement is that when approaching/passing under a lamp the illumination captured by the sensor should change. This fact is in general true since the irradiance E (W/m^2) or illumination (lumen/m^2 = lux) over a surface at a distance R from a lamp, follows the inverse square distance law, i.e. $E = I/R^2$, where I is the radiant intensity (lumen/sr = candela) that emits a source of light. In a typical configuration, with lamps on the ceiling, and a person walking along a horizontal surface (the floor), the distance R between the user and the lamp reach a minimum (the illumination is higher) when the user is under the lamp. The change in the registered illuminance is used to detect the light spot, as explained later in next subsection.

We do not intent to model the radiation pattern of any lamp in the building; apart that it is quite difficult to do it precisely, we do not see it too practical since there are simpler methods to detect light spots, which is our main goal. To get an idea of the complexity of any model, we first have to take into account that the maximum light illuminance that is expected under a light, is ideally modeled by the inverse square distance law, however that basic law is modified by the typical reflectors in common lamps, as well by the lamp diffusers. Other near-by reflectors, such as walls or furniture (mirrors) can influence as well in the perceived illumination from a lamp. Moreover, the output of the illumination sensor depends also on the angle, ϕ, of the sensor's normal with respect to the lamp-to-user axis (see Fig. 5); the Lambert's law states in that case that the illuminance is $E = I \cdot \cos(\phi)/R^2$. This angle ϕ depends not only on the tilt of the sensor but also on the relative position between the sensor and the lamp.

No need to say, that the Light-matching approach can only get benefits when the lamps are switched-on and the light sensor has a Line-of-Sight (LOS) with the lamp (e.g. if using a smartphone as in in Fig. 1). The effect of having some switched-off lights in the building only has the inconvenient of getting less detections, so the number of location hypothesis are pruned more slowly.

2) Light Spot Detection: We use the change in the registered illuminance to detect a light spot. When the user approaches a switched-on lamp the illuminance captured by the light sensor grows, then reaches a maximum when the user gets the closest to the lamp, and finally, as he gets further from the light spot, the illumination decreases again. The ideal peak-like illumination pattern occurs if the user pass exactly under a lamp. However, in order to detect as many light spot as possible, we also desire detections when the user passes close to the lamp (typically about 1 meter). The shape and height of the peak must be processed in order to robustly detect light spots.

The algorithm used for light spot detection consists of the following five stages:

- *Low-Pass Filtering*. We apply a low pass filter to smooth the illuminance sensor values. The smoothing is made with a 4th-order Butterworth Infinity-Impulse-Response (IIR) filter with a cut-off frequency of 1 Hz.

$$E_f(t) = \begin{array}{ll} \sum_{p=0}^{3} E(t-p) * b(p+1) & - \\ \sum_{p=1}^{4} E_f(t-p) * a(p) & , \end{array} \quad (8)$$

where a and b are the coeficients of the filter, and E_f is the filtered illumination. This filter has a phase delay of 4 radians at 1 Hz ($\text{delay}_{\text{filt}} = 4$ rad).

- *Derivative of Illumination*. The derivative of the illumination keeps all the information of a peak and removes the irrelevant constant illumination levels of any particular room. We differentiate consecutive filter illumination values as follows:

$$\dot{E}_f(t) = \begin{cases} \frac{E_f(t)-E_f(t-1)}{T_s} & if E_f(t) \leq 1000 \text{ lux} \\ 0 & \text{otherwise} \end{cases} , \quad (9)$$

where T_s is the sampling interval.

- *Binarization of the Derivative*. We apply a simple thresholding in order to extract the sections where there is an steady illumination grow, and the complementary sections that contain a systematic illumination decrease. The threshold value used to select the relevant changes in illumination is 200 lux/s:

$$\dot{E}_f^{\text{Binary}}(t) = \begin{cases} 1 & if \dot{E}_f(t) \geq 100 \text{ lux/s} \\ -1 & if \dot{E}_f(t) \leq -100 \text{ lux/s} \\ 0 & \text{Otherwise} \end{cases} . \quad (10)$$

- *Peak detection*. A peak corresponds to a zero-crossing in the derivative of the filtered illumination, if it is surrounded at both sides by significant positive and negative illumination gradients. A way to robustly detect this zero-crossing is to check the fulfillment of the next conditions:

$$\text{LD}(t) = \begin{cases} 1 & \text{if } \dot{E}_f^{\text{Binary}}(t) = -1 \ \& \\ & \dot{E}_f^{\text{Binary}}(t-\Delta t) = 0 \ \& \\ & \sum_{i=2}^{w} \dot{E}_f^{\text{Binary}}(t-i\Delta t) > 1 \ \& \\ & \text{SET}_{i=2}^{w}\{\dot{E}_f^{\text{Binary}}(t-i\Delta t) < 0\} = \emptyset \\ 0 & \text{Otherwise} \end{cases} , \quad (11)$$

where w is an integer value representing a window of past illumination samples.

- *Delay compensation*. Since the time t, at which a light spot is detected LD(t), is delayed by the filter and by the binarized zero-crossing, the time $t_{\text{measu}}(k)$ at which the user should have detected the lamp is computed as: $t_{\text{measu}}(k) = t - t_{\text{filter}} - t_{\text{ZC}}$. This corrected time of measurement is used to weight the particles in the PF, by interpolating the particles' state between consecutive step detections using eq. 5.

In Fig. 6 this light spot detection process is shown for some real tests in a building with some fluorescent lamps. In this figure we show the original illumination as captured by the sensor E, all the intermediate processed signals (E_f, $\dot{E}_f$, $\dot{E}_f^{\text{Binary}}(t)$), as well as the time detections.

3) Lamp Database: The lamp database is just a list with the features of each lamp in a building. We annotate its 2D position (r_l), the height with respect to the floor (H_l), the size of the illumination section in terms of its length (L_l) and width (W_l) ($L_l = W_l$ for circular/square lamps), and the orientation (θ_l) of the larger axis of symmetry with respect to the North, i.e. the lamp database contains $\{r_l, H_l, L_l, W_l, \theta_l\}$ for $l = 1 \ldots \text{N}$.

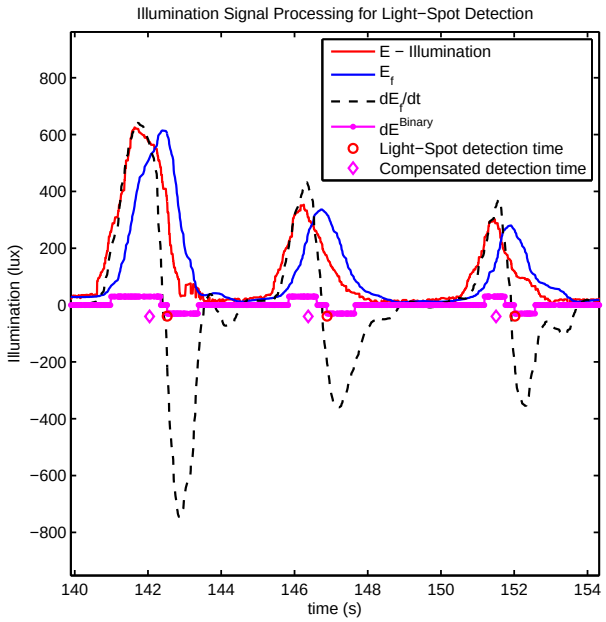

Fig. 6. Processing of the illumination data E to detect light spots. Real example for a person walking at constant speed in a corridor holding a smartphone (Samsung Galaxy S-3) on his hand.

In our current implementation, we do not include any other feature related to the intensity flux of the lamp, as the power, radiant flux lobe, etc.

4) Light Measurement Model: This Light-based measurement model is ambiguous by nature; i.e. when we detect a light spot we know that the user is under a switched-on lamp, but we do not under which particular lamp since they are not codified by any method. Consequently the measurement model is multi modal, i.e. is formed by a mixture of probability distributions centered in the lamp's position. With this measurement model the weight update of each particle in the P.F. is done as follows:

$$w^{(i)}[k] = w^{(i)}[k-1] \cdot P(\text{LD}(t_{\text{measu}}[k])|\hat{r}^{(i)}[k]), \qquad (12)$$

where $P(\text{LD}(t_{\text{measu}}[k])|\hat{r}^{(i)}[k])$ is the probability of getting a light detection ($\text{LD}(t_{\text{measu}}[k] = 1$) when the user is at position $\hat{r}^{(i)}[k]$. This multimodal probability is modeled as the sum of all the probability distributions of each Lamp in a building floor:

$$P(\text{LD}(t_{\text{measu}}[k])|\hat{r}^{(i)}[k]) = \sum_{l=1}^{L} P_l(\text{LD}(t_{\text{measu}}[k])|\hat{r}^{(i)}[k]), \qquad (13)$$

where L is the total number of lights in a floor, l is the index of a particular lamp. We propose to use a standard two-dimensional normal distribution centered at the lamp's position, and with a covariance matrix adapted to the size and orientation of the lamp, in order to model each lamp:

$$P_l(\text{LD}(t_{\text{measu}}[k])|\hat{r}^{(i)}[k]) = \frac{1}{2\pi\sqrt{|\Sigma_l|}} \exp\{-0.5(\hat{r}^{(i)}[\text{k}] - r_l)\Sigma_l^{-1}(\hat{r}^{(i)}[\text{k}] - r_l)^T\}, \qquad (14)$$

where r_l is the position of the l lamp, and Σ_l is a covariance matrix that defines the area around the position of lamp l where is probable to detect it.

C. Additional Measurements Models

In the general localization framework presented in Fig. 3 any additional measurement can be integrated using this general weight update:

$$w^{(i)}[k] = w^{(i)}[k-1] \cdot P(z[k])|\hat{X}^{(i)}[k]), \qquad (15)$$

which is adapted for each particular type of measurement:

- *Magnetometer*. If a magnetometer provides the estimation of the heading of the user θ_{magne} then we can update particle's weight as:

$$P(\theta[k])|\hat{X}^{(i)}[k]) = \exp(-\frac{|\Delta\theta^{(i)}|^2}{2\sigma_m^2}) \qquad (16)$$

  where $\Delta\theta^{(i)} = \theta_{\text{magne}} - X(4)^{(i)}$ and σ_m is the uncertainty of the electronic compass's heading estimation.

- *WiFi/RSS*. Assuming that we measure the signal strength $\text{RSS}[k]$ to an access point, we can update the weights of each particle as:

$$P(\text{RSS}[k])|\hat{r}^{(i)}[k]) = \exp(-\frac{|\Delta\text{RSS}^{(i)}|^2}{2\sigma_{\text{RSS}}^2}) \qquad (17)$$

  where $\Delta\text{RSS}^{(i)} = \text{RSS}[k] - (\text{RSS}_0 - 10\beta\log_{10}(\|\hat{r}^{(i)}[k] - r_{\text{AP}}\|))$ being β the path loss exponent, RSS_0 the expected signal strength at a reference distance of 1 meter, and r_{AP} the position of the WiFi access point ($\sigma_{\text{RSS}} = 6$ dB).

- *Map-matching*. The weight of a particle is set to zero,

$$P(r^{(i)}[j]|r^{(i)}[j], r^{(i)}[j-1]) = 0, \qquad (18)$$

  whenever the segment connecting two consecutive step locations ($r^{(i)}[j]$, $r^{(i)}[j-1]$) intersect any wall of a building floor map.

This section has detailed our particular Light-matching implementation, including the extension for using other sources of information available from unmodified buildings. Next sections evaluate the performance of the Light-matching concept and the benefits of integrating it with complementary signals of opportunity.

IV. Evaluation: Simulated results

A. Convergence of location hypothesis

In section II we analyzed the dependance of the number of location hypothesis with the number of detected lights. We obtained an algebraic expression (eq. 1) that was valid for the case of aligned regular-distributed lamps and for a person walking along a straight path. In this section, we perform several simulations to get an idea of the dependance of the number of hypotheses with the number of light detections in a 2D case, as well as, how the speed of convergence to a single location hypothesis is influenced by the regularity of the lamp distribution, the use of the magnetometer, or other information such as map-matching.

In Fig. 7a and b we can see the simulated environment, which has an area of 98 square meters (14 by 7 meters), a wall distribution that defines a vertically-aligned corridor at the right, and two rooms at the left. There are two different lamp distributions, in Fig.7a 15 lights are distributed regularly with an inter-lamp distance of 2 meters, whereas in Fig.7b the lights are distributed in an irregular way, with different gaps between lamps: 2 and 4 meters, as well as some asymmetries, as the one generated by the three lights at the lower-left room. The simulated walking trajectory is also overlaid on the map in blue color; the crosses represent the stances and the small circle the initial and final position of the path. The trajectory passes under some of the lights in the environment but other lamps are not visited as in a real case. The lengths of the trajectories are long enough so as to obtain 20 light detections in each case.

The evolution of the number of hypotheses for the regular light distribution is shown in Fig.7c. The number of clusters in the arbitrary distribution of particles are calculated automatically using a hierarchical binary tree clustering algorithm, which measures the distance among particles in a space of four dimensions made of these components:$\{r_x^{(i)}, r_y^{(i)}, \cos(\theta^{(i)}), \sin(\theta^{(i)})\}$. Four localization algorithms are compared: 1) the basic *Light-matching* (LM) algorithm (which includes the PDR subsystem), 2) the case of augmenting the LM approach with information from the magnetometer, 3) augmentation by map-matching, and 4) the complete integration with LM plus the magnetometer and map-matching. We can see in Fig. 7c that the initial number of hypotheses is high (larger than the number of lamps) as expected, then after some additional detections the number of hypotheses are decreased. In the LM case, there is no convergence and a minimum of 4 hypothesis persist if no more information is used. The hypothesis converge to two potential locations if the magnetometer or the map is used. However the integration of the whole information makes the location algorithm to converge to a single hypothesis after the ninth light detection.

In the case with an irregular and asymmetrical light distribution, as already expected from the analysis in section II, the convergence is improved significantly (see Fig.7d). Even using the LM method alone, it is possible to find a convergence after the eighth detection. Using some additional information a single hypothesis is obtained after the fifth detection. These simulations, although are just an example of infinite possible configurations, give an approximate idea of how the conver-

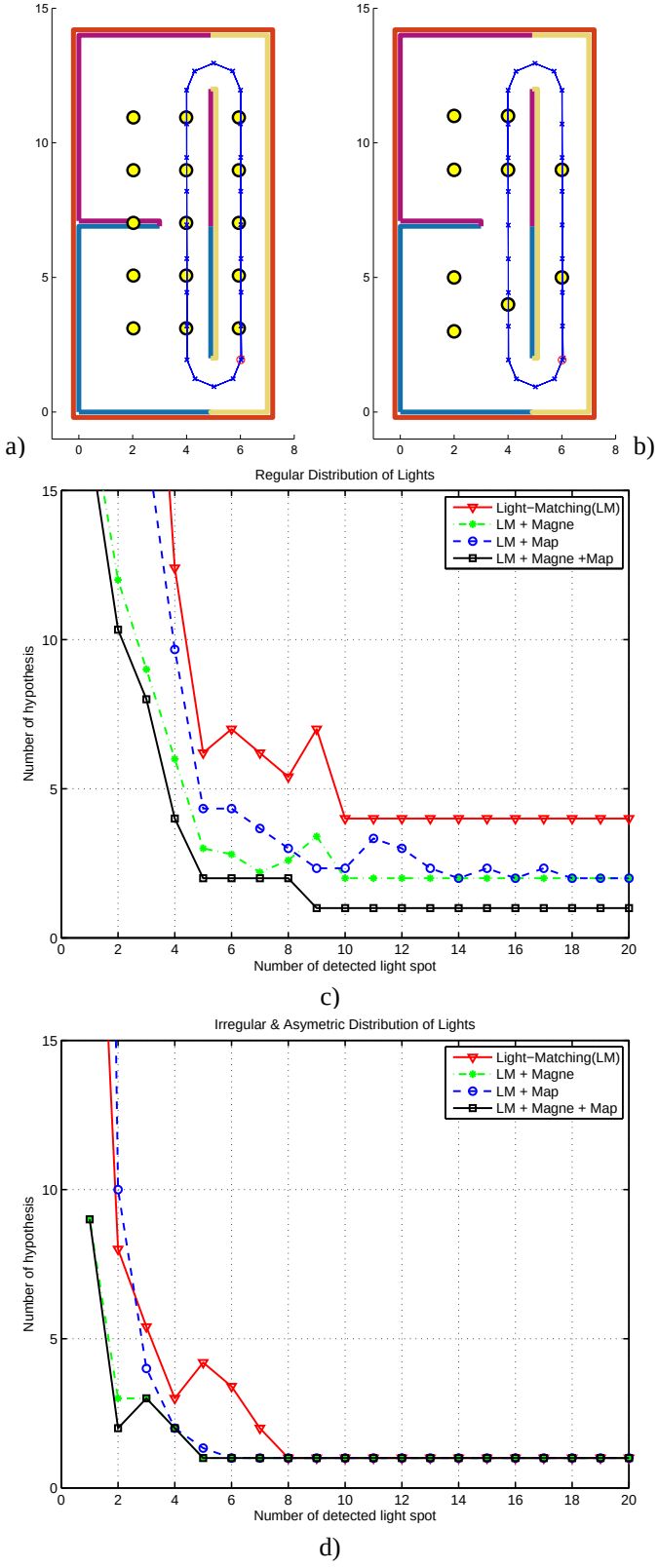

Fig. 7. Simulated analysis in 2D of the dependance of the number of location hypothesis with the number of detected lights. a) Simulated environment with regular light distribution, b) Simulated environment with irregular and asymetrical light distribution, c) Evolution of the number of hypotheses for the regular case, d) Evolution of the number of hypotheses for the other case.

gence is influenced by light distributions and by the addition of extra information. In the real world, we know that we will benefit from irregular light distributions when changing from one room to another, and also from using as many signals of opportunities as possible.

B. Location Accuracy

In order to evaluate the positioning accuracy for the simulated tests, we use a CDF, i.e a Cumulative Density Function, which represents the percentage of location estimations with a positioning error lower than a given value. In these simulations we computed the 2D-positioning error with respect to the ground-truth created to generate the synthetic tests.

The objective is to compare the improvements that can be achieved when using different fusion combinations. First, we tried to evaluate how a WiFi-based positioning solution, assisted with relative Dead-Reckoning information, could be improved when the Light-matching (LM) method was enabled, or when the magnetic information is used. In Fig. 8a we can see how the basic WiFi+PDR fusion approach has an error of 1 meter or lower for 70% of the cases. When the magnetic information is used (WiFi+PDR+Mag) the accuracy is improved significantly ($\leq$ 0.7 m at 70%). When the Light-matching method is used (WiFi+PDR+LM), it is observed an important reduction of the errors, specially at the lowest range of errors. The improvement is similar when adding the magnetometer (WiFi+PDR+LM+Mag). The LM improvement (traces with circle markers in Fig. 8a vs. those with cross markers) is caused by the corrections at light detections that concentrates the particles around a lamp position, resetting any accumulated drift error. Note that many parts of the trajectories (at least 20%) have errors quite larger than 1 meter; these large errors come from the initial sparse distribution of particles around the simulated indoor area, since no initial position nor orientation is given. When enough information is received (from WiFi or Light-detections) the initially spread, or even multimodal, distributions start to concentrate and the accuracy gets lower than 0.3 meters in most of the cases. The benefit of using Light-matching (LM) information is clear in the case of complementing it with WiFi or RSS based positioning methods.

We also analyzed the potential benefit of the LM concept if used in parallel to a Map-matching location method assisted by relative Dead-Reckoning information. In Fig. 8b it can be seen that for this particular simulation, the basic Map-matching with inertial information (Map+PDR) has a poor performance. This is caused by a multimodal particle distribution, in particular two location hypothesis are formed, one of these is the right one and the other is a symmetric and wrong hypothesis. The weighted average of the particles (eq. 7) gives a position estimation close to the center of the indoor area. When we add the magnetic information (Map+PDR+Mag) this ambiguity is eliminated and the location accuracy is very good (lower than 0.9 m in 70% of the cases). The LM approach also eliminated this location ambiguity and the results are similarly good in both cases: without the magnetometer (Map+PDR+LM) and with it (Map+PDR+LM+Mag). As a conclusion, the performance of Map-matching is very good when no symmetries exist in the indoor area; the benefit of LM, as well as of some other sources of information (Magnetometer, WiFi,...), when

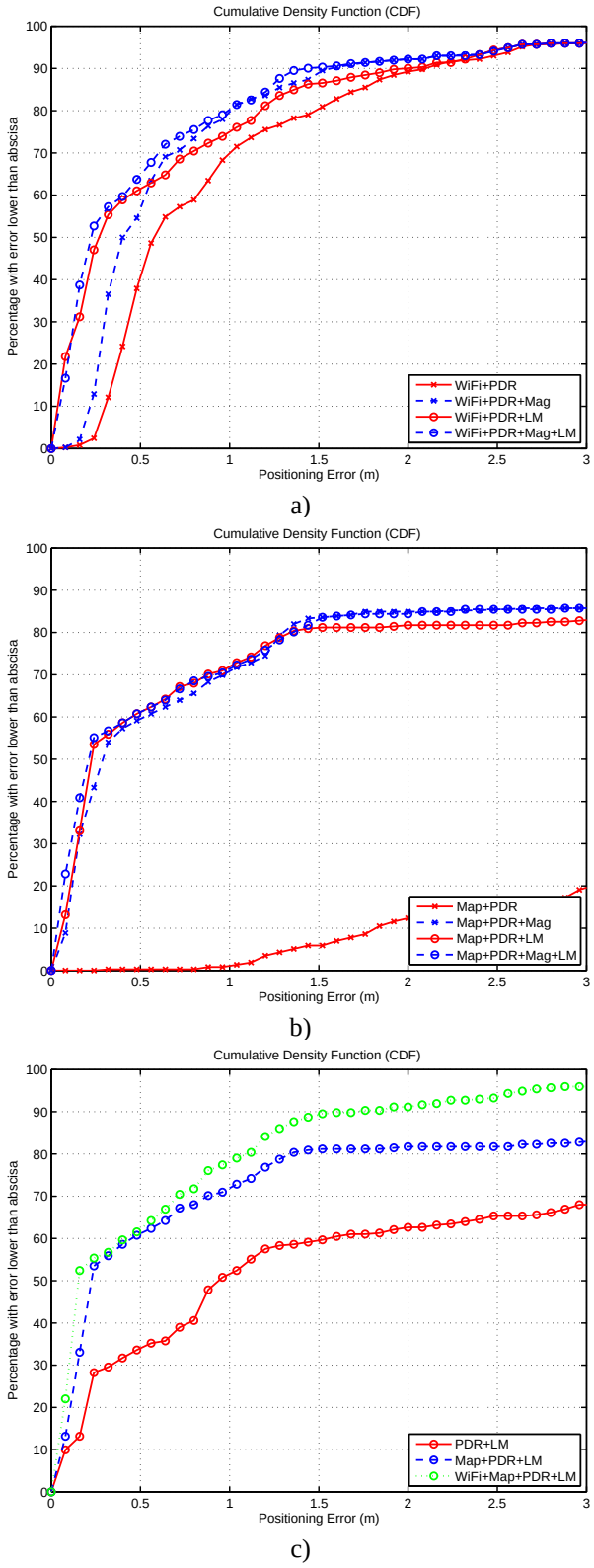

Fig. 8. Positioning accuracy by means of Cumulative Density Functions (CDFs). This data is obtained from some simulated trajectories corresponding to the scenario of Fig.7b. The three CDFs correspond to: a) Benefit obtained in WiFi-based positioning techniques by adding the Light-Matching (LM) method, as well as a magnetometer. b) Benefit obtained in Map-maching-based positioning techniques by adding the Light-Matching (LM) method, as well as a magnetometer. c) Positioning errors with the Light-maching method alone, and the benefits obtained by LM when other methods are fused (Map-matching and WiFi positioning).

compared to the map-matching approach is the improvement of the convergence to an unimodal probability density function.

We finally studied how the basic version of the LM approach (PDR+LM) could be improved by the addition of other sources of information. It is expected a significant improvement, since the LM is a good complement to improve other location method, but is not recommended to work alone, since LM information needs some time to converge and it is not always available (smartphone in the pocket, no lights switched-on, and so on). In Fig. 8c we can see that the CDF of the basic PDR+LM method is, for half of the estimations, not very good (larger than 1 m). This is due to the speed of convergence of this method, as already explained in IV-A. When the Map-matching technique aids the LM alone estimation (Map+PDR+LM) the accuracy gets better than 1 m for 70% of the cases. The usage of an absolute location method such as WiFi-based positioning (WiFi+Map+PDR+LM) helps to reduce the larger errors that are caused by the delay to converge to an uni-modal hypothesis. Note that this convergence problem would normally appear at the beginning of estimations, so for long trajectories or continuous operation, these CDFs would show a better performance as the convergence problem represent a lower percentage of the experiment. As a conclusion, the combination of matching approaches (Light- or Map-based) with absolute positioning techniques is always a good fusion scheme if available, since all methods together eliminate multi-hypothesis and permits to reach sub-meter positioning accuracy.

V. Conclusions

This paper has presented a concept termed as *Light-matching* (LM) which is a new way to use the information coming from unmodified lights in indoor environments to achieve accurate physical location without the need of any illumination-state calibration. As in other matching techniques, we need to know the 2D positions, size and orientation of all lamps in a building, however the current lighting state (if they are on or off) is not needed. The light-matching method also requires the use of an inertial Dead-Reckoning (PDR) method to estimate the displacement and changes in orientation of the person while is walking. Even from an initially unknown location and orientation, whenever the person passes below an switched-on light spot, the location likelihood is iteratively updated until the likelihood potentially converges to a unimodal probability density function. The time to converge to an unimodal position hypothesis depends on the number of lights detected and the asymmetries/irregularities of light distributions. This approach can be used in cooperation with other signals of opportunity (WiFi, Magnetometers or map-maching) to obtain an even better indoor localization accuracy. Apart from giving the basic description of the light-matching concept, we gave the implementation details using a particle filter, and made several simulations to study the convergence and location error of estimations. The performance of the integrated solution achieves a localization error that can be better than 1 m in most of the cases.

Acknowledgment

The authors thank the financial support received from projects: LEMUR (TIN2009-14114-C04-03), LAZARO (CSIC-PIE Ref.201150E039) and LORIS (TIN2012-38080-C04-04).

References

[1] R. Mautz, *Indoor Positioning Technologies*. PhD thesis, 2012.

[2] Y. Gu, A. Lo, and I. Niemegeers, "A Survey of Indoor Positioning Systems for Wireless Personal Networks," *IEEE COMMUNICATIONS SURVEYS & TUTORIALS*, vol. 11, no. 1, pp. 13–32, 2009.

[3] J. Hightower and G. Borriello, "Location Systems for Ubiquitous Computing," *Computer*, vol. 34, no. 8, pp. 57 – 66, 2001.

[4] A. Jiménez, F. Seco, J. Prieto, and J. Guevara, "A comparison of Pedestrian Dead-Reckoning algorithms using a low-cost MEMS IMU," in *2009 IEEE International Symposium on Intelligent Signal Processing*, pp. 37–42, Ieee, Aug. 2009.

[5] R. Mautz, "The challenges of indoor environments and specification on some alternative positioning systems," in *Positioning, Navigation and Communication WPNC'09*, pp. 29–36, 2009.

[6] L. E. Miller, "Indoor Navigation for First Responders : A Feasibility Study," Tech. Rep. February, 2006.

[7] E. Foxlin, "Pedestrian tracking with shoe-mounted inertial sensors," *IEEE Computer Graphics and Applications*, no. December, pp. 38–46, 2005.

[8] R. Feliz, E. Zalama, and J. García-Bermejo, "Pedestrian tracking using inertial sensors," *Journal of Physical Agents*, vol. 3, no. 1, pp. 35–43, 2009.

[9] A. Jiménez, F. Seco, J. Prieto, and J. Guevara, "Indoor Pedestrian Navigation using an INS/EKF framework for Yaw Drift Reduction and a Foot-mounted IMU," in *WPNC 2010: 7th Workshop on Positioning, Navigation and Communication*, vol. 10, pp. 135–143, 2010.

[10] R. Harle, "A Survey of Indoor Inertial Positioning Systems for Pedestrians," *IEEE COMMUNICATIONS SURVEYS & TUTORIALS*, no. December 2012, pp. 1–13, 2013.

[11] A. Jiménez, F. Seco Granja, J. C. Prieto Honorato, and J. Guevara Rosas, "Accurate Pedestrian Indoor Navigation by Tightly Coupling a Foot-mounted IMU and RFID Measurements," *IEEE Transactions on Instrumentation and Measurement*, vol. 61, no. 1, pp. 178–189, 2012.

[12] O. Woodman, "Introduction to Inertial Navigation," Tech. Rep. 03, Cambridge, Jan. 2007.

[13] L. A. Merry, R. M. Faragher, and S. Scheding, "Comparison of Opportunistic Signals for Localisation,"

[14] A. Dammann, S. Sand, and R. Raulefs, "Signals of opportunity in mobile radio positioning," in *2012 Proceedings of the European Signal Processing Conference*, no. Eusipco, pp. 549–553, 2012.

[15] A. Golding and N. Lesh, "Indoor navigation using a diverse set of cheap, wearable sensors," in *Third Int. Symposium on Wearable Computers, (San Francisco)*, pp. 29–36, 1999.

[16] N. Ravi and L. Iftode, "Fiatlux: Fingerprinting rooms using light intensity," in *Adjunct Proceedings of the Fifth International Conference on Pervasive Computing*, 2007.

[17] J. Randall, O. Amft, and M. Burri, "LuxTrace - Indoor Positioning Using Building Illumination," *Personal and Ubiquitous Computing*, vol. 11, no. 6, pp. 417–428, 2007.

[18] M. Nakajima and S. Haruyama, "New indoor navigation system for visually impaired people using visible light communication," *EURASIP Journal on Wireless Communications and Networking*, vol. 2013, no. 1, p. 1, 2013.

[19] M. Ambur, "Indoor positioning and Navigation using Light sensor," *International Journal of Research in Computer and Communication technology*, vol. 2, no. 1, pp. 20–23, 2013.

[20] M. S. Arulampalam, S. Maskell, N. Gordon, and T. Clapp, "A Tutorial on Particle Filters for Online Nonlinear / Non-Gaussian Bayesian Tracking," *IEEE Transactions on Signal Processing*, vol. 50, no. 2, pp. 174–188, 2002.

[21] F. S. Zampella, Alfonso Bahillo, Javier Prieto, Antonio R. Jimenez, "Indoor positioning using Pedestrian Dead Reckoning and RSS / TOF measurements," *Sensors and Actuators A: Physical*, no. to appear soon, pp. 1–7, 2013.